Journal of Physics D: Applied Physics

PAPER

Ultra-broad range organic solid-state laser from a dye-doped holographic grating quasi-waveguide configuration

To cite this article: Minghuan Liu *et al* 2017 *J. Phys. D: Appl. Phys.* **50** 315103

IOP Publishing Journal of Physics D: Applied Physics
J. Phys. D: Appl. Phys. 50 (2017) 315103 (9pp) https://doi.org/10.1088/1361-6463/aa7b59

Ultra-broad range organic solid-state laser from a dye-doped holographic grating quasi-waveguide configuration

Minghuan Liu[1,2], **Yonggang Liu**[1], **Zenghui Peng**[1], **Quanquan Mu**[1], **Zhaoliang Cao**[1], **Xinghai Lu**[1], **Ji Ma**[1] and **Li Xuan**[1,3]

[1] State Key Laboratory of Applied Optics, Changchun Institute of Optics, Fine Mechanics and Physics, Chinese Academy of Sciences, Changchun 130033, People's Republic of China
[2] University of Chinese Academy of Sciences, Beijing 100049, People's Republic of China

E-mail: liuminghuan13@mails.ucas.ac.cn, liuyonggang@ciomp.ac.cn, peng@ciomp.ac.cn, muquanquan@ciomp.ac.cn, caozlok@ciomp.ac.cn, luxh@ciomp.ac.cn, jma2@kent.edu and xuanli@ciomp.ac.cn

Received 17 February 2017, revised 15 May 2017
Accepted for publication 23 June 2017
Published 17 July 2017

CrossMark

Abstract

This paper reports the ultra-broad 149.1 nm lasing emission from 573.2 to 722.3 nm using a simple [4-(dicyanomethylene)-2-methyl-6-(p-dimethylaminostyryl)-4H-pyran] (DCM)-doped holographic polymer-dispersed liquid crystal (HPDLC) grating quasi-waveguide configuration by varying the grating period. The lasing emission beams show *s*-polarization property. The quasi-waveguide structure, which contained the cover glass, the DCM-doped HPDLC grating, the semiconducting polymer film poly[-methoxy-5-(2′-ethyl-hexyloxy)-1,4-phenylene-vinylene] (MEH-PPV), and the substrate were confirmed to decrease lasing threshold and broaden lasing wavelength. The operational lifetime of the device is 240 000 pulses, which corresponds to an overall laser duration of more than 6 h at a repetition rate of 10 Hz. In addition, the dual-wavelength lasing range from the 8th and 9th order is over 40 nm. The electrical tunability of the dual-wavelength lasing emission is over 1 nm. The experimental results facilitated the decreased lasing threshold and broadened lasing wavelength range of organic solid-state lasers.

Keywords: organic solid-state laser, holographic polymer-dispersed liquid crystal, quasi-waveguide configuration, ultra-broad lasing range, tunability

(Some figures may appear in colour only in the online journal)

1. Introduction

Organic solid-state lasers (OSSLs) attract more and more attention and are intensively developed in recent years [1–5]. OSSLs conventionally use a laser dye-doped medium or semiconducting polymer film as an active medium. The configuration such as distributed feedback (DFB), distributed Bragg reflector (DBR), micro-cavity, or multi-dimensional photonic crystal (MPC) was used as a laser oscillation cavity to provide positive feedback for the lasing emission buildup [1, 2]. The promising electrical injection excitation of OSSLs makes them outstanding light sources [6]. The indirect electrical injection excited by light emitting diode (LED) significantly reduces the lasing threshold and immensely advances the industrial application of OSSLs [7, 8].

Unlike inorganic semiconductors [9], organic materials usually possess broad absorbance and photo-luminescent spectra, which provide OSSLs the abilities to radiate laser even in all the visible bands [10, 11]. Doping and blending materials were used to overcome the quenching phenomena of laser dye molecules by Forster transfer to broaden the lasing range of laser dyes [12, 13]. Schneider *et al* reported the 115.3 nm lasing emission from 597.8 nm to 713.1 nm by doping 4-(dicyanomethylene)-2-methyl-6-(julolidin-4-yl-vinyl)-4H-pyran (DCM_2) into the

[3] Author to whom any correspondence should be addressed.

host materials tris-(8-hydroxy-quinoline)aluminum (Alq3) and varying the grating period [10]. Oussama Mhibik *et al* demonstrated 230 nm broad lasing emission using five kinds of laser dye molecules and a blending system [11]. However, the lasing range reported in the literature is insufficiently broad, and the doping and blending method are complicated and ineffective. Therefore, searching for a simple method to broaden the lasing range of OSSLs is urgent.

This study demonstrated the ultra-broadly tunable 149.1 nm lasing emission (from 573.2 nm to 722.3 nm) from the laser dye [4-(dicyanomethylene)-2-methyl-6-(p-dimethylaminostyryl)-4H-pyran] (DCM) by varying the grating period (from 550 nm to 710 nm) of the holographic polymer-dispersed liquid crystal (HPDLC). The DCM laser dye was added into the pre-polymer mixture in the material preparation period and stabilized into the HPDLC grating as emitters during excitation. The high refractive index semiconducting polymer film poly[-methoxy-5-(2′-ethyl-hexyloxy)-1,4-phenylene-vinylene] (MEH-PPV) was sandwiched between the HPDLC layer and the glass substrate. The quasi-waveguide device configuration, which contained a cover glass, HPDLC layer, MEH-PPV film, and substrate glass, was confirmed to decrease the lasing threshold of the DCM-doped HPDLC distributed feedback (DFB) laser and to broaden the lasing range. The emission beam polarization property, the device's operational lifetime, and the dual-wavelength tunability were demonstrated. In addition, the dual-wavelength lasing, which was achieved from the 8th and 9th diffraction orders, possessed a lasing range of over 40 nm. The device, which possesses the advantages of lightweight, ease of fabrication, cost-effectiveness, broad lasing, and dual-wavelength lasing range, can be used as smart light sources.

2. Experiment

2.1. Material and sample preparation

The pre-polymer mixture was created to fabricate polymer-dispersed liquid crystal (PDLC) and HPDLC film [14]. The mixture contained 58.5 wt.% photo-sensitive acrylate monomers (dipentaerythritol hydroxyl pentaacrylate (DPHPA, Aldrich)), 29.3 wt.% non-reactive liquid crystals (TEB-30A, $n_o = 1.522$, $n_e = 1.692$, Silichem), 9.8 wt.% crosslinking agent N-vinylpyrrolidone (NVP, Aldrich), 0.5 wt.% photoinitiator Rose Bengal (RB, Aldrich), 1.4 wt.% coinitiator N-phenylglycine (NPG, Aldrich), and the laser dye DCM (Aldrich, 0.5 wt.%). The mixture was stirred for 48 h in a sealed-in glass bottle to obtain an isotropic and homogeneous material system.

The MEH-PPV (OLED) film was coated onto a clean glass substrate by spin-casting from the MEH-PPV/tetrahydrofuran (THF) solution at 0.8 wt.% as the high refractive index layer [15, 16]. The sample cell consisted of two pieces of glass substrates: one had a spin-coating MEH-PPV film and the other was a pure glass. The sample cell gap thickness was controlled at 9 μm by spacers. The mixture was infiltrated into the sample cell via capillary force in a darkroom. The refractive index of the DCM-doped pre-polymer mixture after illumination is 1.536 at 589 nm (2WA, Kernco). The refractive index of the MEH-PPV is 2.0 at 589 nm [17].

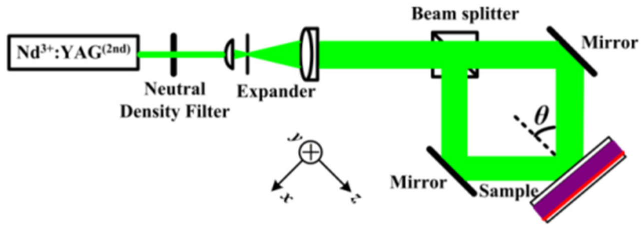

Figure 1. Schematic experimental setup for the HPDLC grating fabrication.

For absorbance and photoluminescence (PL) spectra, the laser dye DCM was doped into the isotropic and homogeneous DPHA/NVP (6:1 by weight) mixture with a weight ratio of 0.5 wt.%. The DCM-doped mixture was infiltrated into a 9 μm glass cell without an MEH-PPV film coating. The absorbance spectrum of the DCM-doped sample was performed by UV–VIS spectrometer (UV-3101PC, SHIMADZU), and the PL spectrum was conducted using F-7000FL (Hitachi) spectrometer. The excitation wavelength was 470 nm for the PL spectrum to match the maximum absorbance of the laser dye DCM.

2.2. HPDLC grating fabrication

The oscillation cavity HPDLC grating was fabricated via polymerization-induced phase separation (PIPS) [14]. The schematic experimental setup is shown in figure 1, and the details can be found elsewhere [15]. A conventional two-beam interference configuration was used to illuminate the sample in order to fabricate HPDLC grating as shown in figure 1. The 532 nm line of a primary continuous *s*-polarized neodymium-doped yttrium aluminum garnet (Nd^{3+}:YAG) laser (New Industries Optoelectronics) beam was expanded and spatially filtered to deliver a uniform plane wave, and the primary laser beam was then split into two coherent objects and reference beams. Interference between the beams formed a two-beam interference pattern, which was recorded by the pre-polymer mixture. The recording beams initially passed through the pre-polymer mixture and then to the MEH-PPV film. The recording time is 3 min for every sample. The period Λ is mainly determined by the writing wavelength λ_{rec} and half of the intersection angle θ of the writing beams expressed as follows:

$$\Lambda = \frac{\lambda_{rec}}{2\sin(\theta)}. \tag{1}$$

The fascinating nature for HPDLC grating is that different grating periods can be easily obtained by simply varying the intersection angle in the experiments. Therefore, the grating period can be selected to match the gain spectrum of the laser active medium in order to provide lasing emission operation [3, 18].

2.3. Lasing excitation

For lasing excitation, the samples were transversely optical excited by the 532 nm line of a frequency doubled Q-switched

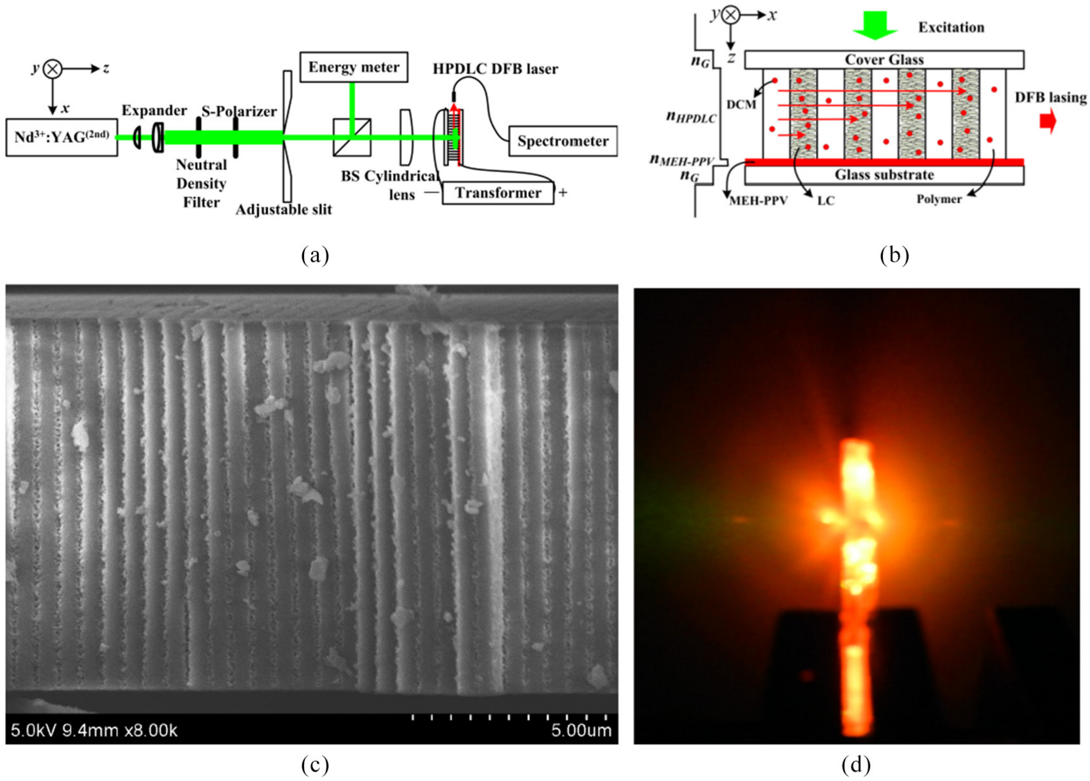

Figure 2. Lasing excitation experiments. (a) Schematic of the experimental setup for transverse lasing excitation, (b) device structure for quasi-waveguide configuration HPDLC DFB laser, (c) side view SEM of the HPDLC grating with the grating period at 596 nm, and (d) emission pattern of the quasi-waveguide configuration HPDLC DFB laser collected by a digital camera with the excitation energy at 30 μJ/pulse.

Nd^{3+}:YAG pulsed laser, which delivered a pulse duration at 10 ns and repetition at 10 Hz (second harmonic generation [19], New Industries Optoelectronics), as shown in figure 2(a). The output lasing emission was collected from the HPDLC DFB laser sample edge with a fiber-coupled grating spectrometer (Sofn Instruments). The resolution limit of the detection system is 0.25 nm. The excitation energy was monitored by the redirect part of the incident energy via a non-polarized beam splitter (NPBS) in real time. The incident excitation beam was expanded using an expander. After which, an adjustable slit filtered the central part of the incident excitation beam to ensure uniform pumping. In addition, the excitation beam was reshaped with a cylinder lens ($f = 200$ mm) to produce a 3 by 1 mm excitation beam. Moreover, an s-polarizer was used to polarize the incident excitation laser beam. A variable neutral density filter was used to regulate the pump energy to investigate output-emission intensity as a function of excitation energy. To investigate the electrical field-induced tunability, a variable transformer was used to apply electric field to the HPDLC DFB lasers with indium tin oxide (ITO)-coated glass cells.

Figure 2(b) shows the device configuration. The device consisted of the cover glass, the DCM-doped HPDLC grating layer, the high refractive index semiconducting polymer film MEH-PPV, and the glass substrate. The encapsulated device configuration can prevent photo-induced degradation and oxidation, which helps improve photo-stability [20]. The refractive index of the PDLC film after photo-illumination is 1.536 at 589 nm. The PDLC film with LC molecules oriented randomly in the polymer matrix was obtained by illuminating the pre-polymer mixture with single laser beam. The device configuration created a quasi-waveguide structure because the refractive index of the lasing emission layer was lower than that of the polymer film MEH-PPV [21]. The scanning electron microscope (SEM, Hitachi S-4800) image for HPDLC grating with the period at 596 nm is shown in figure 2(c). The SEM image confirmed that the HPDLC grating contains alternative polymer and firm LC layers. Figure 2(d) shows the emission pattern for the quasi-waveguide configuration HPDLC DFB laser collected by a digital camera (Nikon, S-9100) with the excitation energy at 30 μJ/pulse.

3. Results and discussions

3.1. Lasing mechanism

For the dye-doped 1D HPDLC DFB laser [22], the density of states $D(\omega)$ at the band edge is expressed as follows:

$$D(\omega) \propto \int \mathrm{d}k\delta(\omega - \omega(k)) = \left|\frac{\mathrm{d}\omega}{\mathrm{d}k(\omega)}\right|^{-1} = \frac{1}{v_{\mathrm{g}}}, \quad (2)$$

where v_{g} is the group velocity. The group velocity approaches zero for the lasing modes near the band edge resulting in singularities in the density of states. Therefore, the spontaneous emission near the band edge is intensively enhanced for the lasing emission to occur when the threshold is reached. Thus, the gain spectrum overlap of the laser dye DCM with the density of states determines the occurrence of gain amplification. The lasing wavelength λ_{las} in a vacuum for dye-doped HPDLC DFB laser [15, 23] is determined by

$$\lambda_{\text{las}} = \frac{2n_{\text{eff}}\Lambda}{m}, \quad (3)$$

where n_{eff} is the effective refractive index of the lasing wavelength, Λ is the period of the HPDLC grating, and m is the diffraction order. For the first order HPDLC ($m = 1$), the value of n_{eff} is 1.536, and the shortest wavelength ($\theta = 90°$) we can obtain is 815 nm. However, the 815 nm laser cannot operate. According to equation (3), the grating period is 198 nm to emit laser at 610 nm for the first order HPDLC. However, according to equation (1), the smallest grating period we can obtain is 266 nm; therefore, the first order HPDLC is unreasonable to be used as a laser oscillation cavity in this work. Different lasing wavelengths can be obtained by selecting various grating periods. The feedback for HPDLC DFB laser was provided by backward Bragg scatterings and distributed throughout the excitation zone as shown in figure 2(b) [24]. The lasing emission was collected from the sample edge with transverse photo-pumping as shown in figure 2(a). The excitation beams initially passed through the DCM-doped HPDLC grating and then the MEH-PPV film.

3.2. Spectroscopic characterization of the laser dye DCM

For the laser dye DCM, the luminescence will be reabsorbed by another molecule leading to the luminescence emission quenches [25]. Therefore, this study used 0.5 wt.% laser dye DCM to decrease the molecule density in the medium in order to prevent concentration quenching. The laser dye DCM possesses visible broad photoluminescence (PL) spectra, which can facilitate laser emission within the broad PL spectrum as shown in figure 3. The full width at half maximum (FWHM) for the PL spectrum is 90 nm. Different diffraction order and grating period can be selected to detect the lasing emission according to equation (3). The absorbance and PL peaks are around 470 and 580 nm. The absorbance for wavelengths over 570 nm is sufficiently weak as shown in figure 3. Therefore, lasing emission should occur when the cavity mode is selected to emit laser around 570 nm according to equation (3). The narrow band spectrum, which possesses the FWHM at 9 nm and centers around 610 nm, is the amplified spontaneous emission (ASE) [26, 27] spectrum. The ASE was collected from the DCM-doped PDLC sample edge, representing the position for the largest net gain (gain center). The PDLC sample was fabricated by irradiating the pre-polymer mixture with single laser beam. The excited light wave is amplified when it travels along the waveguide and guided to the edge during the transverse excitation process. Therefore, ASE occurs when gain overcomes losses, e.g. net gain.

3.3. Lasing properties for quasi-waveguide configuration

Figure 4 compares the emission wavelength and conversion for the waveguide and quasi-waveguide configuration, e.g. the device without and with MEH-PPV film. The conversion is the slope conversion efficiency when excitation energy exceeds lasing threshold. For the waveguide configuration HPDLC DFB laser, the DCM-doped HPDLC is sandwiched between two pure low refractive index glasses. The thickness of the MEH-PPV is around 150 nm, which is controlled by the spin speed and measured by a surface profiler (KLA Tencor P-16+). In our previous work, we reported the lasing emission from MEH-PPV film [15, 16]. Good lasing emission occurred when the thickness of MEH-PPV film was 75 nm, e.g. the lasing emission from the MEH-PPV film depended on its thickness. A 150 nm thickness is selected to suppress the lasing emission from the MEH-PPV layer. Both central lasing emission wavelengths for the devices with waveguide and quasi-waveguide configurations located at 610 nm are shown in figure 4(a). The excitation energy is 6 μJ/pulse for the waveguide and quasi-waveguide configuration HPDLC DFB lasers. The uniform of the central lasing emission wavelength confirms that the introduction of the MEH-PPV film has no influence to the device central wavelength. The diffraction order is 3rd, and the grating period is selected at 596 nm to obtain lasing emission at 610 nm, which is in the central range of the ASE spectra. The effective refractive index for lasing emission at 610 nm is 1.535. The FWHM for the 610 nm lasing emission is 0.42 and 0.85 nm for the device with quasi-waveguide and waveguide configurations, respectively. The experimental results indicate that the quasi-waveguide configuration HPDLC DFB laser shows an advantage for spectral compression than the device with waveguide configuration. In addition, the 0.42 nm FWHM of the lasing emission spectrum confirms the excellent spectra selection and compression for the HPDLC DFB laser in comparison with the ASE (9 nm) and PL (90 nm) spectra. The lasing threshold for the device with waveguide and quasi-waveguide configurations is shown in figure 4(b). The lasing threshold is 0.9 and 2.6 μJ/pulse for the device with quasi-waveguide and waveguide configurations, respectively. The experimental results confirmed that the introduction of MEH-PPV film can help decrease lasing threshold and improve device conversion.

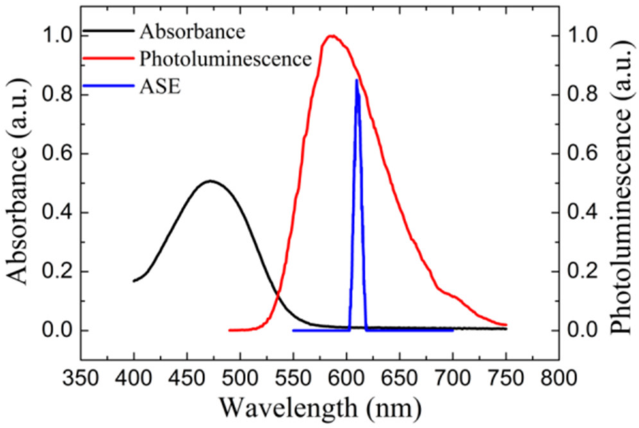

Figure 3. Absorbance, photoluminescence, and ASE spectra of the laser dye DCM.

The gain properties for the waveguide and quasi-waveguide configuration devices can be determined by using the

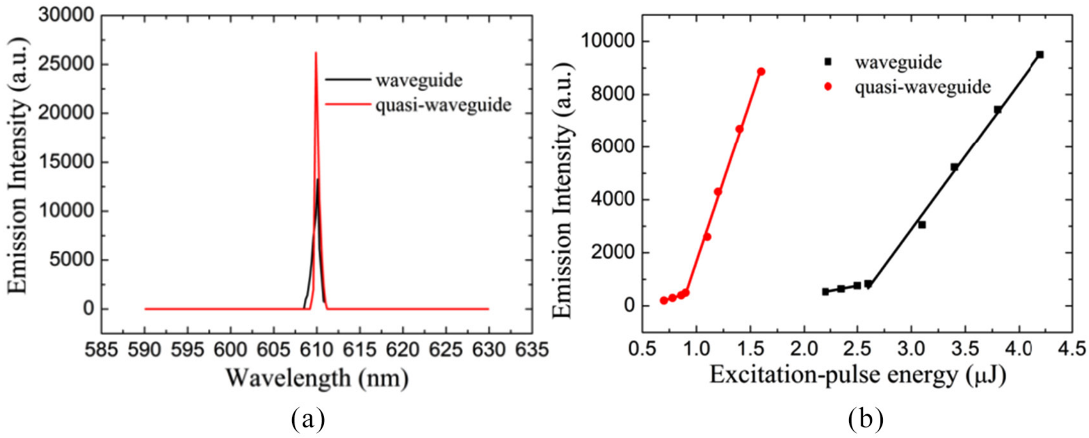

Figure 4. Comparison of lasing characterizations for the waveguide and quasi-waveguide configuration HPDLC DFB lasers. (a) Emission intensity as functions of wavelength and (b) excitation-pulse energy. The circular points are experimental data, and the lasing threshold can be determined from the linear fits.

variable stripe length method (VSL) [26, 27]. For gain properties, the DCM-doped PDLC layer was fabricated for waveguide and quasi-waveguide configurations. The ASE occurs when gain exceeds losses during the transverse excitation. When exciting the sample with a variable stripe length, the ASE intensity from the PDLC sample edge should be governed by the following:

$$I = \frac{AI_p}{g}\left[e^{gl} - 1\right], \tag{4}$$

where A is a constant related to the spontaneous emission cross section, I_p is the excitation intensity, g is the net gain parameter, and l is the excitation stripe length. Figure 5 shows the dependence of the emission intensity at 610 nm on the excitation stripe length with an excitation intensity of 70 kW cm^{-2}. The net gains are 13.5 and 21.6 cm^{-1} for the DCM-doped waveguide and quasi-waveguide configurations, respectively. Therefore, net gain properties further confirm that the waveguide configuration has advantages over the waveguide configuration. A larger net gain helps decrease the threshold for laser operation. Thus, it is deduced that the quasi-waveguide configuration HPDLC DFB laser can emit laser in a range broader than the waveguide configuration.

The polarization property of the lasing emission beams from the 610 nm lasing quasi-waveguide configuration HPDLC DFB laser is shown in figure 6(a). A polarizer was inserted into the laser sample and the spectral collection system for polarization property characterization. Emission intensity fits the cosine line shape well, and the polarization ratio is as high as 94%, which demonstrates that the lasing emission beams are s-polarization. The device operational lifetime, defined as the lasing emission intensity decaying to half of the initial, is 240 000 pulses with an excitation energy of 30 μJ/pulse for the 610 nm laser as shown in figure 6(b). The 240 000-pulse operational lifetime corresponds to an overall laser duration of 6.6 h. The operational lifetime is higher than that reported with a semiconducting polymer as the active medium, which confirms that the device is photo-stable [28, 29]. The emission pattern from the quasi-waveguide configuration HPDLC DFB laser is shown in figure 2(d). In our previous report, we

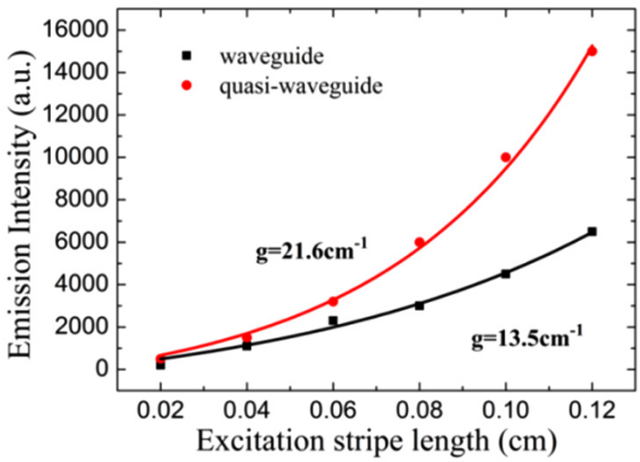

Figure 5. Dependence of the emission intensity at 610 nm on the excitation stripe length with an excitation intensity of 70 kW cm^{-2}. The solid lines fit the data using equation (4), and the net gain of the waveguide and quasi-waveguide configurations can be determined from the fits.

demonstrated lasing emissions from different orders with MEH-PPV as the active medium. The emission pattern is fan-shaped [15]. However, the fan-shaped emission pattern does not occur in this study, as shown in figure 2(d), which confirms that the 150 nm-thick MEH-PPV film inhibits the lasing emission from the MEH-PPV layer.

3.4. Ultra-broad lasing range for the quasi-waveguide configuration HPDLC DFB laser

The ultra-broad 149.1 nm lasing emission that ranged from 573.2 nm to 722.3 nm for the quasi-waveguide configuration HPDLC DFB laser is shown in figure 7(a). The thickness of the MEH-PPV film is around 150 nm. The lasing range was just 67 nm (from 590 nm to 657 nm) with MEH-PPV film used as the active medium [15]. In this regard, the 149.1 nm lasing emission range using DCM as the active medium confirms the advantage of the quasi-waveguide configuration. The diffraction order is 3rd for lasing wavelength at 573.2, 577.4,

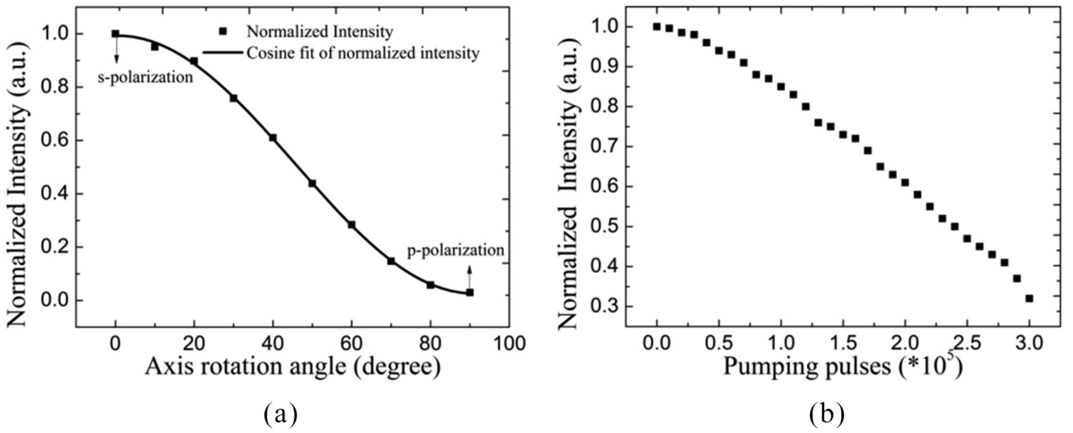

Figure 6. Lasing properties for the quasi-waveguide configuration HPDLC DFB laser. (a) Normalized intensity as a function with the polarizer axis rotation angle. The emission intensity from different angle is normalized with the s-polarization intensity, and the fit is cosine. (b) Normalized intensity as a function with pumping pulses.

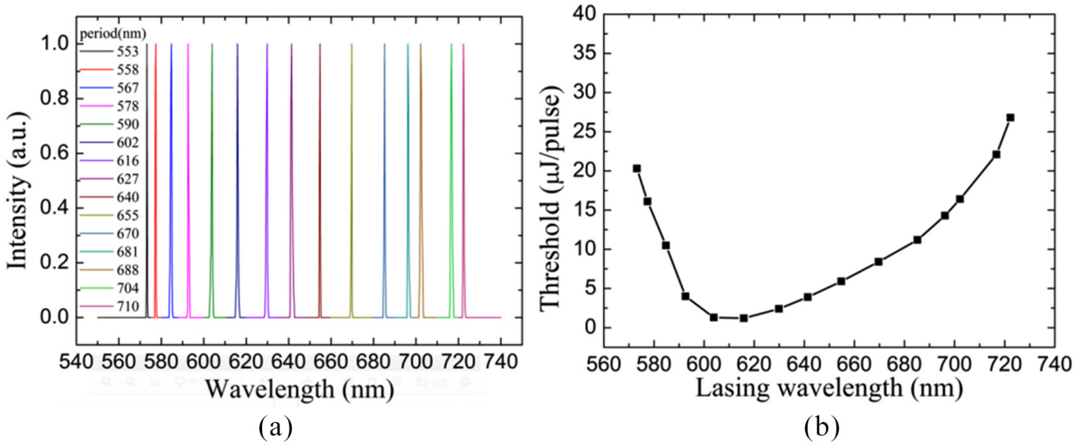

Figure 7. Ultra-broad range quasi-waveguide configuration HPDLC DFB laser. (a) Normalized lasing spectra as a function of wavelength from different grating periods and (b) lasing threshold at different lasing wavelengths for the quasi-waveguide configuration HPDLC DFB laser.

584.8, 592.6, 603.9, 615.9, 629.9, 641.4, 654.8, 669.7, 685.2, 696.2, 702.2, 716.7, and 722.3 nm. In addition, the grating period is selected at 553, 558, 567, 578, 590, 602, 616, 627, 640, 655, 670, 681, 688, 704, and 710 nm to emit laser at 573.2, 577.4, 584.8, 592.6, 603.9, 615.9, 629.9, 641.4, 654.8, 669.7, 685.2, 696.2, 702.2, 716.7, and 722.3 nm, respectively. The recording intensity for the grating period at 553, 558, 567, 578, 590, 602, 616, 627, 640, 655, 670, 681, 688, 704, and 710 nm is 3.8, 3.6, 3.42, 3.3, 3.13, 3.06, 3.01, 2.95, 2.9, 2.85, 2.8, 2.75, 2.7, 2.65, and 2.6 mW cm^{-2}, respectively. The effective refractive index is 1.555, 1.551, 1.547, 1.538, 1.535, 1.535, 1.535, 1.534, 1.534, 1.534, 1.533, 1.533, 1.531, 1.527, and 1.525 for 573.2, 577.4, 584.8, 592.6, 603.9, 615.9, 629.9, 641.4, 654.8, 669.7, 685.2, 696.2, 702.2, 716.7, and 722.3 nm lasing, respectively. The 149.1 nm lasing emission from single laser dye DCM using a simple quasi-waveguide structure is the broadest in the literature [10]. The lasing range is from 580 nm to 680 nm with waveguide configuration. Therefore, the simple quasi-waveguide configuration can broaden the lasing emission range with the dye-doped waveguide configuration, especially in the red portion. Lasing emission can occur with a thickness from 60 nm to 500 nm. The lasing threshold for the 573.2, 577.4, 584.8, 592.6, 603.9, 615.9, 629.9, 641.4, 654.8, 669.7, 685.2, 696.2, 702.2, 716.7, and 722.3 nm lasing emission is 20.3, 16.1, 10.5, 4, 1.3, 1.2, 2.4, 3.9, 5.9, 8.4, 11.2, 14.3, 16.4, 22.1, and 26.8 μJ/pulse, respectively, as shown in figure 7(b). The experimental results indicate that the lasing wavelength has lower threshold around the ASE spectra as shown in figure 7(b) because the net gain is larger around the ASE spectra [26, 27]. No lasing emission over 722.3 nm is found because the net gain is insufficient to support the lasing emission oscillation buildup. In addition, the absorbance is so strong that lasing emission cannot occur below 573.2 nm. Widely tunable laser sources in the visible range of the spectrum are required for many applications such as spectroscopy or sensing [30, 31]. The ultra-broad range organic solid-state laser demonstrates a simple and cost-effective solution, which provides tunable visible coherent radiation in comparison to the complex and expensive optical parametric oscillators (OPOs) or generators in this work [32, 33]. Two or three kinds of organic solid-state lasers provide the lasing emission to cover the whole visible

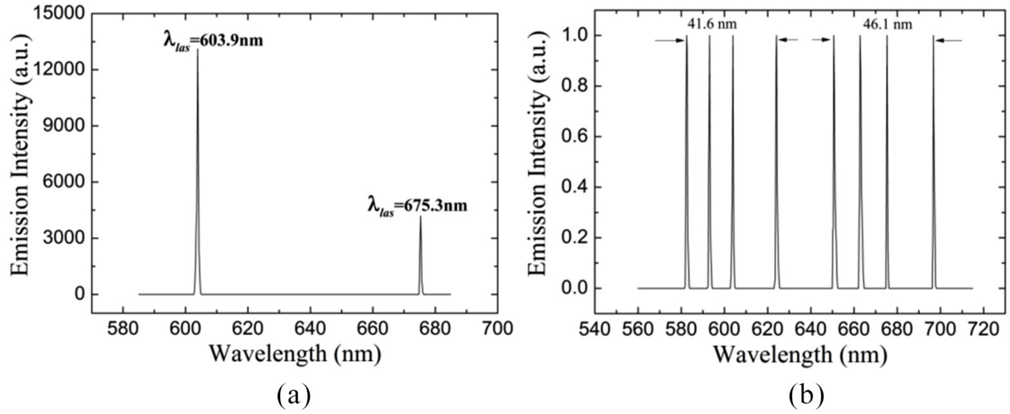

Figure 8. Dual-wavelength lasing quasi-waveguide configuration HPDLC DFB laser. (a) Dual-wavelength lasing emission intensity as a function of wavelength with the grating period at 1.71 μm and (b) dual-wavelength lasing range for the quasi-waveguide configuration HPDLC DFB laser by changing the grating period.

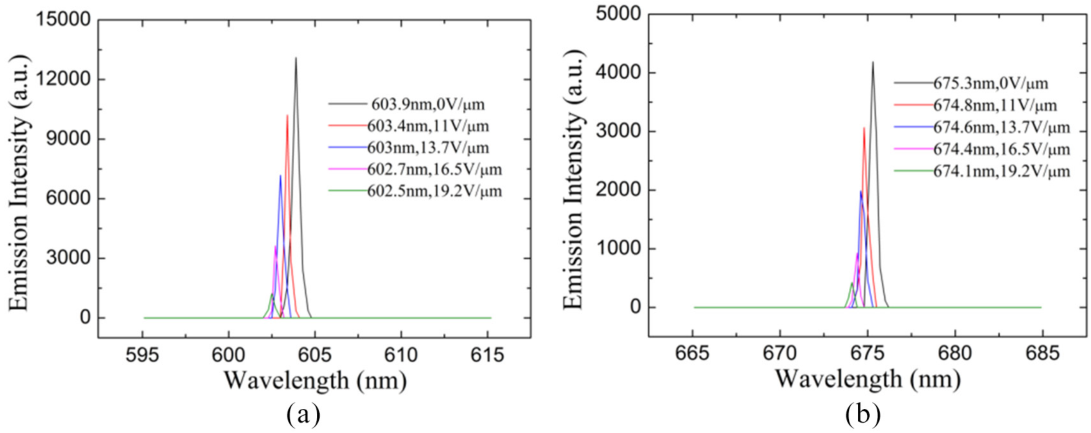

Figure 9. Electric field-induced tunability of the dual-wavelength lasing quasi-waveguide configuration HPDLC DFB laser. The emission intensity as a function of the wavelength with variable electric field for (a) 603.9 and (b) 675.3 nm lasing.

range in comparison to the narrow band inorganic semiconductor laser diode [34].

3.5. Dual-wavelength lasing for the quasi-waveguide configuration HPDLC DFB laser

Dual-wavelength lasing emission can occur when different cavity modes exist in the gain spectra for different adjacent orders according to equation (3) [35], e.g. the dual-wavelength lasing emission operates when a specialized grating period is selected. Figure 8(a) shows the dual-wavelength lasing emission spectra for the quasi-waveguide configuration HPDLC DFB laser. The thickness for the MEH-PPV film is 150 nm, and the recording intensity is about 2.8 mW cm^{-2}. The lasing wavelengths, which center at 603.9 and 675.3 nm, are from the 8th and 9th diffraction order, respectively. In addition, the grating period is selected at 1.71 μm to achieve the dual-wavelength lasing emission for the quasi-waveguide configuration HPDLC DFB laser. The effective refractive index is 1.585 and 1.575 for 603.9 and 675.3 nm lasing, respectively. The reason that the intensity for 603.9 nm lasing emission at an excitation energy of 50 μJ/pulse is higher than 675.3 nm lasing emission that the 603.9 nm lasing emission possesses a larger net-gain and a lower lasing threshold. Figure 8(b) shows the dual-wavelength lasing emission range for the quasi-waveguide configuration HPDLC DFB laser. The lasing emission centers at 582.5, 593.1, 603.9, and 624.1 nm for the 9th order and the lasing emission centers at 650.6, 662.8, 675.3, and 696.7 nm for the 8th order. The grating period is selected at 1.65, 1.68, 1.71, and 1.77 μm to achieve lasing emission at 582.5, 593.1, 603.9, and 624.1 nm, respectively. The effective refractive index is 1.588, 1.586, 1.585, 1.583, 1.576, 1.575, 1.575, and 1.571 for 582.5, 593.1, 603.9, 624.1, 650.6, 662.8, 675.3, and 696.7 nm lasing, respectively. The lasing range is over 40 nm from the 8th and 9th orders for the quasi-waveguide configuration HPDLC DFB laser. The broad dual-wavelength lasing range confirms the advantage of the quasi-waveguide configuration HPDLC DFB laser.

Lasing emission can be tuned when the effective refractive index n_{eff} varies with external stimulations from equation (3) [36–38]. Thanks to the positive nematic LC in HPDLC grating, which is sensitive to the electric field, the lasing emission of the HPDLC DFB laser can be tuned as LC is reoriented in this context [39]. The tunable nature is appealing and fascinating in the fields of sensing and spectroscopy [30, 31]. The electric field-induced tunability of the dual-wavelength lasing quasi-waveguide configuration HPDLC DFB laser is illustrated in figure 9. Narrow peaks and spectra are observed in each case which indicates that lasing emission remains satisfactory. Emission intensity decreases with electric field because of the decrease of the refractive index modulation between the polymer layer and the LC layer with the reorientation of the LC, which promotes the lasing threshold. The lasing emission wavelength is 603.4, 603, 602.7, and 602.5 nm with the electric field at 11, 13.7, 16.5, and 19.2 V μm^{-1} for the 603.9 nm lasing emission as shown in figure 9(a), respectively. Therefore, the tunable range is as high as 1.4 nm. The blue shift of the lasing emission is attributed to the decrease in the effective refractive index of the lasing mode when applying electric field. Accordingly, the change of the effective refractive index is 3.7×10^{-3}. Lasing wavelength is 674.8, 674.6, 674.4, and 674.1 nm with the electric field at 11, 13.7, 16.5, and 19.2 V μm^{-1} for the 675.3 nm lasing emission as shown in figure 9(b), respectively. As a result, the tunable range is 1.2 nm, which corresponds to the change in the effective refractive index at 2.8×10^{-3} according to equation (3). The tunable range for the 675.3 nm lasing emission is shorter than that of the 603.9 nm lasing emission because the material refractive index dispersion is smaller at 675.3 nm. The quasi-waveguide configuration HPDLC DFB laser device, which possesses the advantages of electrical tunability, broad lasing, and dual-wavelength lasing range, can be used as smart light sources.

4. Conclusions

In summary, we demonstrated the ultra-broad lasing range 149.1 nm lasing emission from 573.2 nm to 722.3 nm from the simple DCM-doped HPDLC grating quasi-waveguide configuration by varying the grating period. The operational lifetime of the device is 240 000 pulses, corresponding to an overall laser duration of more than 6 h at a repetition rate of 10 Hz. The emission beams show good *s*-polarization property. The quasi-waveguide structure, which contained the cover glass, the DCM-doped HPDLC grating, the semiconducting polymer film MEH-PPV, and the substrate, was confirmed to decrease lasing threshold and broaden lasing wavelength. In addition, the dual-wavelength lasing range from the 8th and 9th order is over 40 nm. The experimental results pave a simple means of decreasing the lasing threshold and broadening the lasing wavelength of OSSLs. The quasi-waveguide configuration HPDLC DFB laser device, which possesses the advantages of light-weight, ease of fabrication, cost-effectiveness, tunability, broad lasing emission, and dual-wavelength lasing range, can be used as smart light sources.

Acknowledgment

We thank Zhongxu Cui and Shu Pei of the State Key Laboratory of Applied Optics for the helpful discussion and film thickness testing.

Funding

This work is supported by the National Natural Science Foundation of China (61377032, 61378075).

References

[1] Samuel I D W and Turnbull G A 2007 Organic semiconductor lasers *Chem. Rev.* **107** 1272–95
[2] Chenais S and Forget S 2012 Recent advances in solid-state organic lasers *Polym. Int.* **61** 390–406
[3] Llobera A, Juvert J, Gonzalez-Fernandez A, Ibarlucea B, Carregal-Romero E, Buttgenbach S and Fernandez-Sanchez C 2015 Biofunctionalized all-polymer photonic lab on a chip with integrated solid-state light emitter *Light Sci. Appl.* **4** e271
[4] Vannahme C, Dufva M and Kristensen A 2015 High frame rate multi-resonance imaging refractometry with distributed feedback dye laser sensor *Light Sci. Appl.* **4** e269
[5] Mhibik O, Forget S, Ott D, Venus G, Divliansky I, Glebov L and Chenais S 2016 An ultra-narrow linewidth solution-processed organic laser *Light Sci. Appl.* **5** e16026
[6] Zhang Y F and Forrest S R 2011 Existence of continuous-wave threshold for organic semiconductor lasers *Phys. Rev.* B **84** 241301
[7] Herrnsdorf J *et al* 2013 Micro-led pumped polymer laser: a discussion of future pump sources for organic lasers *Laser Photon. Rev.* **7** 1065
[8] Tsiminis G, Wang Y, Kanibolotsky A L, Inigo A R, Skabara P J, Samuel I D W and Turnbull G A 2013 Nanoimprinted organic semiconductor laser pumped by a light-emitting diode *Adv. Mater.* **25** 2826–30
[9] Son J H, Cho B, Hong S, Lee S H, Hoxha O, Haack A J and Lee L P 2015 Ultrafast photonic Pcr *Light Sci. Appl.* **4** e280
[10] Schneider D *et al* 2004 Ultrawide tuning range in doped organic solid-state lasers *Appl. Phys. Lett.* **85** 1886–8
[11] Mhibik O, Leang T, Siove A, Forget S and Chenais S 2013 Broadly tunable (440–670 nm) solid-state organic laser with disposable capsules *Appl. Phys. Lett.* **102** 041112
[12] Berggren M, Dodabalapur A and Slusher R E 1997 Stimulated emission and lasing in dye-doped organic thin films with forster transfer *Appl. Phys. Lett.* **71** 2230–2
[13] Kozlov V G *et al* 1998 Study of lasing action based on forster energy transfer in optically pumped organic semiconductor thin films *J. Appl. Phys.* **84** 4096–108
[14] Bunning T J, Natarajan L V, Tondiglia V P and Sutherland R L 2000 Holographic polymer-dispersed liquid crystals (H-Pdlcs) *Annu. Rev. Mater. Sci.* **30** 83–115
[15] Liu M H, Liu Y G, Zhang G Y, Peng Z H, Li D Y, Ma J and Xuan L 2016 Organic holographic polymer dispersed liquid crystal distributed feedback laser from different diffraction orders *J. Phys. D: Appl. Phys.* **49** 465102
[16] Huang W, Diao Z, Liu Y, Peng Z, Yang C, Ma J and Xuan L 2012 Distributed feedback polymer laser with an external feedback structure fabricated by holographic polymerization technique *Org. Electron.* **13** 2307–11
[17] Tammer M and Monkman A P 2002 Measurement of the anisotropic refractive indices of spin cast thin poly(2-Methoxy-5-(2′-Ethyl-Hexyloxy)-P-Phenylenevinylene) (Meh-Ppv) films *Adv. Mater.* **14** 210–2
[18] Samuel I D W, Namdas E B and Turnbull G A 2009 How to recognize lasing *Nat. Photonics* **3** 546–9
[19] Manaka T and Iwamoto M 2016 Optical second-harmonic generation measurement for probing organic device operation *Light Sci. Appl.* **5** e16040
[20] Foucher C, Guilhabert B, Herrnsdorf J, Laurand N and Dawson M D 2014 Diode-pumped, mechanically-flexible

polymer DFB laser encapsulated by glass membranes *Opt. Express* **22** 24160–8
[21] Costela A, García O, Cerdán L, García-Moreno I and Sastre R 2008 Amplified spontaneous emission and optical gain measurements from pyrromethene 567-doped polymer waveguides and quasi-waveguides *Opt. Express* **16** 7023–36
[22] Jakubiak R, Bunning T J, Vaia R A, Natarajan L V and Tondiglia V P 2003 Electrically switchable, one-dimensional polymeric resonators from holographic photopolymerization: a new approach for active photonic bandgap materials *Adv. Mater.* **15** 241–4
[23] Riechel S, Lemmer U, Feldmann J, Benstem T, Kowalsky W, Scherf U, Gombert A and Wittwer V 2000 Laser modes in organic solid-state distributed feedback lasers *Appl. Phys.* B **71** 897–900
[24] Kogelnik H and Shank C V 1971 Stimulated emission in a periodic structure *Appl. Phys. Lett.* **18** 152–4
[25] Cornil J, Beljonne D, Calbert J P and Bredas J L 2001 Interchain interactions in organic Pi-conjugated materials: impact on electronic structure, optical response, and charge transport *Adv. Mater.* **13** 1053–67
[26] McGehee M D, Gupta R, Veenstra S, Miller E K, Diaz-Garcia M A and Heeger A J 1998 Amplified spontaneous emission from photopumped films of a conjugated polymer *Phys. Rev.* B **58** 7035
[27] Dal Negro L, Bettotti P, Cazzanelli M, Pacifici D and Pavesi L 2004 Applicability conditions and experimental analysis of the variable stripe length method for gain measurements *Opt. Commun.* **229** 337–48
[28] Persano L, Camposeo A, Del Carro P, Solaro P, Cingolani R, Boffi P and Pisignano D 2009 Rapid prototyping encapsulation for polymer light-emitting lasers *Appl. Phys. Lett.* **94** 123305
[29] So H, Watanabe H, Yahiro M, Yang Y, Oki Y and Adachi C 2011 Highly photostable distributed-feedback polymer waveguide blue laser using spirobifluorene derivatives *Opt. Mater.* **33** 755–8
[30] Liu X *et al* 2015 Tailored surface-enhanced Raman nanopillar arrays fabricated by laser-assisted replication for biomolecular detection using organic semiconductor lasers *ACS Nano* **9** 260–70
[31] Woggon T, Klinkhammer S and Lemmer U 2010 Compact spectroscopy system based on tunable organic semiconductor lasers *Appl. Phys.* B **99** 47–51
[32] Mhibik O, My T-H, Paboeuf D, Bretenaker F and Drag C 2010 Frequency stabilization at the Kilohertz level of a continuous intracavity frequency-doubled singly resonant optical parametric oscillator *Opt. Lett.* **35** 2364–6
[33] Forget S, Balembois F, Lucas-Leclin G, Druon F and Georges P 2003 Picosecond laser source at 1 MHz with continuous tunability in the visible red band *Opt. Commun.* **220** 187–92
[34] Tilma B W, Mangold M, Zaugg C A, Link S M, Waldburger D, Klenner A, Mayer A S, Gini E, Golling M and Keller U 2015 Recent advances in ultrafast semiconductor disk lasers *Light Sci. Appl.* **4** e310
[35] Diao Z H, Deng S P, Huang W B, Xuan L, Hu L F, Liu Y G and Ma J 2012 Organic dual-wavelength distributed feedback laser empowered by dye-doped holography *J. Mater. Chem.* **22** 23331–4
[36] Huang W, Diao Z, Yao L, Cao Z, Liu Y, Ma J and Xuan L 2013 Electrically tunable distributed feedback laser emission from scaffolding morphologic holographic polymer dispersed liquid crystal grating *Appl. Phys. Express* **6** 022702
[37] Diao Z H, Huang W B, Peng Z H, Mu Q Q, Liu Y G, Ma J and Xuan L 2014 Anisotropic waveguide theory for electrically tunable distributed feedback laser from dye-doped holographic polymer dispersed liquid crystal *Liq. Cryst.* **41** 239–46
[38] Zhang G Y *et al* 2016 Tunable surface-emitting dual-wavelength laser from a blended gain layer with an external holographic grating feedback structure *Opt. Mater. Express* **6** 3320–9
[39] Diao Z, Kong L, Xuan L and Ma J 2015 Electrical control of the distributed feedback organic semiconductor laser based on holographic polymer dispersed liquid crystal grating *Org. Electron.* **27** 101–6